Kinetics of tungsten low-pressure chemical-vapor deposition using WF_6 and SiH_4 studied by *in situ* growth-rate measurements

J. A. M. Ammerlaan, P. J. van der Put, and J. Schoonman
Laboratory for Inorganic Chemistry, Delft University of Technology, Julianalaan 136, 2628 BL Delft, The Netherlands

(Received 5 February 1992; accepted for publication 6 January 1993)

The kinetics of tungsten low-pressure chemical-vapor deposition (LPCVD) using WF_6 and SiH_4 have been studied in a vertical hot-wall reactor equipped with a microbalance. *In situ* growth-rate measurements were performed by monitoring the sample weight during tungsten film deposition. The kinetics of the LPCVD process appear to be determined by the ratio of the partial pressures of SiH_4 and WF_6. At low SiH_4/WF_6 ratios, i.e., $p(SiH_4)/p(WF_6) < 0.3$, the kinetics are first and zeroth order with respect to $p(SiH_4)$ and $p(WF_6)$, respectively. At higher ratios, i.e., $0.5 < p(SiH_4)/p(WF_6) < 1.0$, the deposition rate is second and minus first order with respect to $p(SiH_4)$ and $p(WF_6)$, respectively. In both kinetic regimes a zeroth-order dependence on $p(H_2)$ was observed. The growth rate does not vary substantially in the temperature range 200–400 °C. Maximum rate values are observed near 300 °C. An attempt has been made to interpret the observed kinetic behavior in terms of a Langmuir–Hinshelwood model. The proposed surface reaction mechanism involves reaction between chemisorbed SiH species and chemisorbed WF_6 molecules. Different surface reaction pathways, governed by different rate-limiting steps, have been proposed in order to explain the observed kinetics in the two regimes.

I. INTRODUCTION

Tungsten offers several advantages for use in integrated circuit metallization. Low-pressure chemical-vapor deposition (LPCVD) using tungsten hexafluoride (WF_6) as a tungsten source has been proven a promising deposition technique for this application.[1–3] However, selective tungsten LPCVD by hydrogen reduction of WF_6 suffers from a high reactivity of WF_6 toward the silicon substrate, causing Si consumption, encroachment at the Si/SiO_2 interface, and wormhole formation in contact regions. Kusumoto *et al.*[4] have shown that these adverse effects can be circumvented by using silane (SiH_4) as a reducing agent for WF_6. Moreover, selective deposition can be obtained in this process.

From mass spectroscopy and x-ray photoelectron spectroscopy studies Yu, Eldridge, *et al.*[5,6] concluded that reduction of WF_6 by SiH_4 can be expressed as

$$2WF_6+3SiH_4 \rightarrow 2W+3SiF_4+6H_2. \quad (1)$$

However, *in situ* infrared spectroscopy by Kobayashi, Goto, and Suzuki[7,8] indicated that SiF_4 only represents a minor reaction product, whereas most of the SiH_4 is converted to $SiHF_3$,

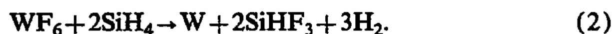

$$WF_6+2SiH_4 \rightarrow W+2SiHF_3+3H_2. \quad (2)$$

An important feature of the SiH_4-based process is the possibility of obtaining high deposition rates at relatively low temperatures (300 °C) compared to conventional tungsten CVD employing reduction of WF_6 by H_2.

Only a few studies dealing with the kinetics of tungsten CVD using SiH_4 and WF_6 have appeared in the literature;[4,9–12] however, the reported film growth rates and the dependence of growth rate on process parameters as temperature and reactant partial pressures show considerable difference. These results were obtained from deposition experiments using cold-wall reactors and *ex situ* film thickness measurements; however, the use of cold-wall-type CVD systems may have disadvantages in kinetic studies. Depletion of reactant gases may result from unfavorable flow patterns and/or temperature gradients in combination with relatively high reactant conversion on large deposition areas. Moreover, measurement and control of wafer temperature may be difficult in these systems.

In the present work, tungsten LPCVD from WF_6 and SiH_4 has been studied using a vertical hot-wall reactor specially designed for investigating the kinetics of this process. The reactor is equipped with a microbalance enabling *in situ* growth rate measurements by monitoring the substrate weight during tungsten film deposition. Care has been taken to avoid limitation of the growth rate by gas-phase transport processes. The present investigation is focused on the determination of the influence of temperature and partial pressures of SiH_4, WF_6, and H_2 on the film deposition rates. The results provide insight into the reaction mechanisms involved in this process, and possible reaction pathways will be discussed.

II. EXPERIMENT

The LPCVD setup designed for growth rate measurements is shown schematically in Fig. 1. It comprises a 26-mm-diam quartz tube in a vertically positioned furnace. Silicon substrates (10×15 mm^2) were cut from (100)-oriented double-side-polished 3 in. wafers (130–160 Ω cm). The substrates were cleaned in fuming HNO_3 and hot concentrated HNO_3 (65%), respectively, before receiving a buffered hydrofluoric acid (BHF) dip to remove

 0021-8979/93/094631-06$06.00 © 1993 American Institute of Physics

Downloaded 22 Feb 2005 to 130.161.132.34. Redistribution subject to AIP license or copyright, see http://jap.aip.org/jap/copyright.jsp

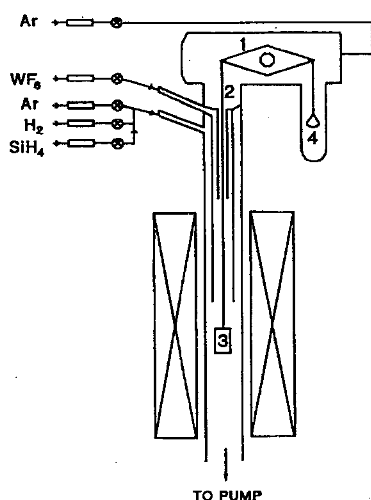

FIG. 1. Schematical presentation of the vertical hot-wall CVD reactor with microbalance. 1: microbalance; 2: Pt wire; 3: Si substrate; 4: counterweight.

native silicon oxide prior to the deposition experiments. The samples were attached to 0.3-mm-diam platinum wires from the microbalance. The microbalance (C.I. Electronics, type MK 2) was operated in the weight ranges 0–20 or 0–200 mg, depending on the accuracy required. The analogue balance signal is converted to a digital weight value monitored by a computer. The weight resolution is 1 μg for the 20 mg range and 10 μg for the 200 mg range.

The reactant gases WF_6 (flow range 2.5–50 sccm, 99.999% purity), SiH_4 (flow range 2.5–50 sccm, Semicon quality), and H_2 (flow range 0–140 sccm, 99.9999% purity) as well as the purging and diluent gas Ar (total range 80–320 sccm, 99.9999% purity) are adjusted by mass flow controllers. To ensure that the measurements are performed in the surface reaction-rate-limited regime, WF_6 and SiH_4 are not premixed before entering the furnace zone. A gas supply arrangement for these reactants by means of concentric tubes minimizes reactant consumption due to deposition on the reactor wall before the substrate is reached. The temperature ranges from 145 to 390 °C, and is measured using a thermocouple positioned near the substrate. Low pressure is maintained by a combination of a Root's pump and a rotary vane pump.

After loading the sample, purging the reactor tube, and heating to the desired temperature, the reactant gases are introduced. Once the pressure and the flow rate are stable, the measurement is performed by monitoring the sample weight while the deposition proceeds. Typical measurement time is 2–5 min, during which the total weight increase amounts to 1–40 mg, depending on process parameters.

The film growth rate was calculated from the constant slope of the plot of weight increase versus time assuming the deposit to have tungsten bulk density (19.3 g/cm^3). Crystalline phases in the deposited films were identified from x-ray-diffraction patterns.

III. RESULTS

A. Reactor performance

Weight measurements before and after the deposition experiments indicated that more than 95% of the weight increase was due to deposition on the silicon substrate, whereas the remaining part was deposited on the Pt wire.

In order to determine the character of the deposition regime governing the system, the total flow rate was varied while total pressure, temperature, and flow ratio of the different feed gases were kept at constant values. On increasing the flow rate a region is entered in which the growth rate is almost independent of the total gas flow. In this regime the deposition rate is assumed to be controlled by surface reaction kinetics rather than gas-phase transport processes. The measurements presented in this article have been performed in the flow-rate-independent deposition regime.

Absence of rate limitations by gas-phase diffusion has also been confirmed by varying the total pressure at constant flow rate, keeping partial pressure values of WF_6 and SiH_4 constant. Lowering the total pressure from 500 to 300 mTorr did not result in a significant increase of the growth rate. Most of the rate measurements presented in this article were carried out at a total pressure of 500 mTorr, permitting large variations in gas flow rate. Moreover, the estimated conversion of reactant gases was less than 10%, also confirming the differential character of the system.

Although linear gas flow velocities are high (10–20 m/s) due to small reactor dimensions and low reactor pressure, the Reynolds numbers are sufficiently low ($Re < 20$) to assure a laminar flow pattern in the reactor tube.

B. Film structure

The structure of the deposited films depends on the ratio of partial pressures of SiH_4 and WF_6. X-ray-diffraction patterns indicated the formation of polycrystalline tungsten with the α (bcc) structure at partial pressure ratios of SiH_4 and WF_6 lower than one. However, increasing the ratio to values higher than one resulted in the formation of a mixture of α-W and β-W. Similar behavior in cold-wall reactors has been reported by Schmitz, Buiting, and Ellwanger[13] and Suzuki *et al.*[14] Deposition of β-W is undesirable since this phase has a considerably higher resistivity than α-W. The requirement of α-W formation restricted the process parameter window in this investigation to ratios of SiH_4 and WF_6 lower than one.

C. Kinetic measurements

The kinetic investigation of the CVD process comprised a systematic variation of the deposition temperature and partial pressures of silane $p(SiH_4)$, tungsten hexafluoride $p(WF_6)$, and hydrogen $p(H_2)$, respecting the boundary condition $p(SiH_4)/p(WF_6) < 1$ as explained in the previous section.

The dependence of the growth rate on $p(SiH_4)$ at 310 °C is shown in Fig. 2. From this plot the kinetic behavior of SiH_4 appears to be influenced by $p(WF_6)$. At

Downloaded 22 Feb 2005 to 130.161.132.34. Redistribution subject to AIP license or copyright, see http://jap.aip.org/jap/copyright.jsp

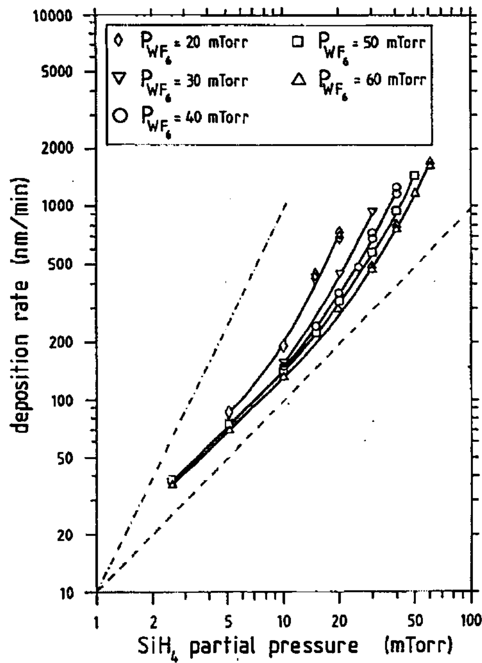

FIG. 2. Tungsten film deposition rate as a function of SiH_4 partial pressure for different WF_6 partial pressures. Measurements performed at 310 °C and 500 mTorr total pressure. Dashed lines indicate slopes corresponding to first (-----) and second (-·-·-·-) -order kinetics.

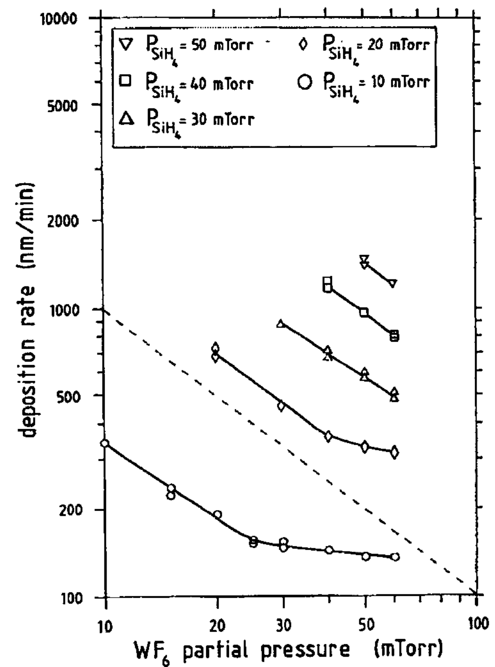

FIG. 3. Tungsten film deposition rate as a function of WF_6 partial pressure for different SiH_4 partial pressures. Measurements performed at 310 °C and 500 mTorr total pressure. The dashed line (-----) indicates a slope corresponding to minus-first-order kinetics.

$p(WF_6)=60$ mTorr a linear increase of the rate with increasing $p(SiH_4)$ is observed until $p(SiH_4)=20$ mTorr. On further increasing $p(SiH_4)$ the dependence changes from linear to quadratic, as is illustrated by the dashed lines in Fig. 2 representing linear and quadratic behavior. The transition from first- to second-order kinetics with respect to $p(SiH_4)$ is also observed at lower $p(WF_6)$. However, the $p(SiH_4)$ range in which this transition takes place moves to lower values, i.e., at $20<p(SiH_4)<30$ mTorr if $p(WF_6)=60$ mTorr, at $15<p(SiH_4)<25$ mTorr if $p(WF_6)=50$ mTorr, at $10<p(SiH_4)<20$ mTorr if $p(WF_6)=40$ mTorr, and at $5<p(SiH_4)<10$ mTorr if $p(WF_6)=20$ mTorr. The highest growth rate obtained in these experiments approaches 1.8 μm/min. This value is considerably higher than values observed in processes using H_2 as a reducing agent.

The dependence of the deposition rate on $p(WF_6)$ is shown in Fig. 3. From this plot it is evident that the dependence is affected by $p(SiH_4)$. At $p(SiH_4)=10$ mTorr the growth rate decreases linearly with increasing $p(WF_6)$ until $p(WF_6)=30$ mTorr, as illustrated by the dashed line in Fig. 3. A further increase of $p(WF_6)$ shows a flattening of the curve and a regime is entered in which the growth rate does not depend on $p(WF_6)$. The transition from minus first order to zeroth order in $p(WF_6)$ takes place at $p(WF_6)=30$ mTorr if $p(SiH_4)=10$ mTorr and at $p(WF_6)=50$ mTorr if $p(SiH_4)=20$ mTorr. At higher $p(SiH_4)$ no order transition is observed below $p(WF_6)=60$ mTorr. The same dependence on $p(WF_6)$ has been observed for $p(SiH_4)=20$ mTorr at 240, 270, and 340 °C. Since the measured deposition rates at these temperatures are nearly equal to those at 310 °C, they have not been included in the plot for the sake of clarity.

In contrast to $p(SiH_4)$ and $p(WF_6)$, the magnitude of $p(H_2)$ has no influence on the deposition rate. Figure 4

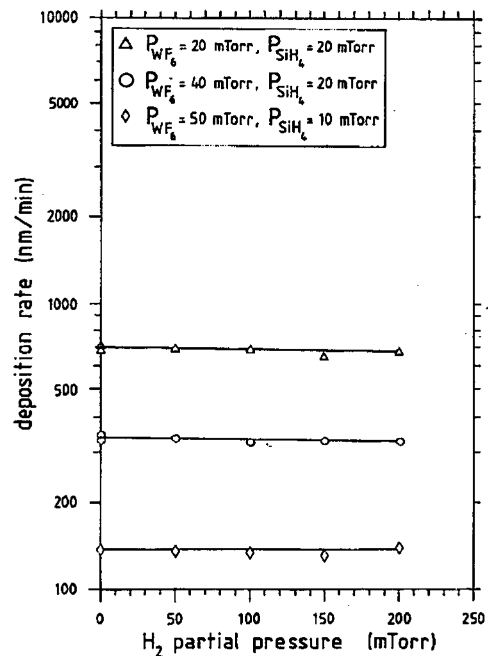

FIG. 4. Tungsten film deposition rate as a function of H_2 partial pressure for different combinations of SiH_4 and WF_6 partial pressures. Measurements performed at 310 °C and 500 mTorr total pressure.

Downloaded 22 Feb 2005 to 130.161.132.34. Redistribution subject to AIP license or copyright, see http://jap.aip.org/jap/copyright.jsp

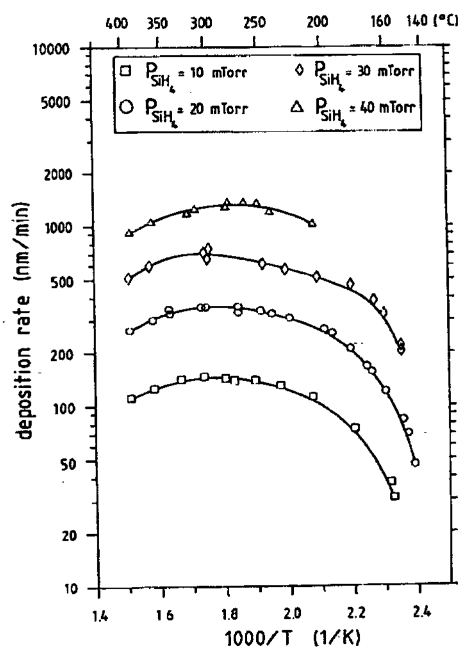

FIG. 5. Tungsten film deposition rate as a function of reciprocal temperature for different combinations of SiH_4 and WF_6 partial pressures. Measurements performed at 500 mTorr total pressure.

shows that the rate does not change significantly in the range $0<p(H_2)<200$ mTorr. This zeroth-order dependence is found in all kinetic regimes.

The influence of temperature on the deposition rate seems rather unusual. Deposits have been obtained at temperatures as low as 145 °C. The rate increases as the temperature is raised. However, in the semilogarithmic plot of rate versus reciprocal temperature in Fig. 5 no lines of constant slope are obtained, which precludes determination of an apparent activation energy for the deposition process from these plots. Moreover, the curves show maximum values of the deposition rate near 300 °C. Decreasing rates are observed above 300 °C. Due to film adhesion failure and concomitant surface increase during deposition, reliable measurements below 200 °C at $p(SiH_4)/p(WF_6)=1$ were not possible.

IV. DISCUSSION

A. Kinetics of film deposition

From the results of the deposition rate measurements, collected in Figs. 2–5, two kinetic regimes can be distinguished in the range of operating conditions considered here. The different expressions for the growth rate dependence on process parameters are

$$R_I=k_I\{T\}[p(SiH_4)]^1[p(WF_6)]^0[p(H_2)]^0 \tag{3}$$

and

$$R_{II}=k_{II}\{T\}[p(SiH_4)]^2[p(WF_6)]^{-1}[p(H_2)]^0. \tag{4}$$

R_I and R_{II} represent the tungsten deposition rates, and $k_I\{T\}$ and $k_{II}\{T\}$ the temperature-dependent reaction rate constants in the respective regimes. Equation (3) matches the observed kinetics if $p(SiH_4)/p(WF_6)<0.3$ (region I), whereas Eq. (4) applies if $0.5<p(SiH_4)/p(WF_6)<1.0$ (region II).

Comparison of the results presented in this work with those reported in the literature shows a considerable difference in kinetic behavior of SiH_4 and WF_6. In most of the cold-wall studies[9–11] the observed orders with respect to $p(SiH_4)$ and $p(WF_6)$ were first and zeroth (or slightly negative, i.e., -0.2) order, respectively, covering the entire range $0<p(SiH_4)/p(WF_6)<1$. The reported growth rates are lower than the rates obtained in our work, thus indicating the occurrence of growth-rate limitation by gas-phase transport of SiH_4 to the substrate surface, consequently resulting in a linear dependence of the rate on the inlet partial pressure of SiH_4. However, in the pioneering work of Kusumoto *et al.*[4] a trend was observed that shows agreement with our results. Although the reactant partial pressures are probably lower in their work, an order with respect to SiH_4 suddenly increasing from first to second was encountered at $p(SiH_4)/p(WF_6)\cong 0.5$. Although the authors did not note this in their article, it is clear from their plot of growth rate versus WF_6 flow rate that the order with respect to WF_6 changes from zeroth to a negative value at $p(SiH_4)/p(WF_6)>0.5$, thus showing the same trend as in our work.

The reported effect of temperature on the rate agrees with our observations. The rate does not change dramatically in the temperature range of 200–400 °C, and a decrease between 300 and 400 °C has also been found by others.[4,10] The small apparent activation energies reported in three studies[11,12,15] have probably been measured in the gas-phase transport-limited regime.

B. Surface reaction mechanism

The transition in reaction orders with respect to $p(SiH_4)$ and $p(WF_6)$, as described in the previous subsection, may indicate that the rate-determining step involved in region I is different from the reaction controlling the deposition rate in region II. Formulated within the framework of the Langmuir–Hinshelwood mechanism, as presented below, a change of rate determining step within a single reaction pathway could be an explanation in case of decreasing reaction orders. However, increasing orders, as observed in this work, indicate the presence of at least two parallel reaction pathways, governing regions I and II, respectively. Each reaction pathway has its own rate-determining step, resulting in different kinetic dependences on reactant partial pressures. Consequently, a proposed surface reaction mechanism of tungsten deposition from SiH_4 and WF_6 should account for the presence of different pathways, predict their kinetic behavior, and account for their respective domination in the observed kinetic regimes. Arora and Pollard[16] have shown the possibility of determining major reaction pathways and rate-determining steps in tungsten CVD from WF_6/H_2 mixtures. Using statistical thermodynamics, transition state theory, and bond dissociation enthalpies, they calculated the rate constants for all possible elementary surface reactions, thus obtaining a detailed set of kinetic parameters. Extension of this pro-

Downloaded 22 Feb 2005 to 130.161.132.34. Redistribution subject to AIP license or copyright, see http://jap.aip.org/jap/copyright.jsp

cedure to predict the kinetics of tungsten CVD from $SiH_4/WF_6/H_2$ mixtures would be more complicated and is beyond the scope of this work. Therefore, less detailed models for heterogeneous reaction kinetics are proposed here. Although less quantitative, these may serve as a first approximation to provide more insight into the surface mechanisms.

We have attempted to interpret our observations on the basis of a Langmuir–Hinshelwood-type model. The procedure involves postulating a series of elementary reactions, subsequently assuming the forward and backward rate to be high enough for all steps to attain equilibrium, except for one step which is considered to be rate limiting. The model comprises adsorption of the reactant molecules SiH_4 and WF_6 on the tungsten surface, subsequent dissociation of adspecies at the surface, and finally formation and desorption of the main reaction product $SiHF_3$ [Eq. (2)]:

$$SiH_4(g)+2^*\leftrightarrows SiH_3^*+H^*, \tag{5}$$

$$SiH_3^*+{}^*\leftrightarrows SiH_2^*+H^*, \tag{6}$$

$$SiH_2^*+{}^*\leftrightarrows SiH^*+H^*, \tag{7}$$

$$2H^*\leftrightarrows H_2(g)+2^*, \tag{8}$$

$$WF_6(g)+{}^*\leftrightarrows WF_6^*, \tag{9}$$

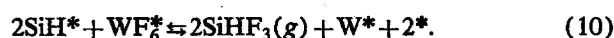

$$2SiH^*+WF_6^*\leftrightarrows 2SiHF_3(g)+W^*+2^*. \tag{10}$$

In these equations the asterisk symbolizes a free surface site, i.e., a surface tungsten atom capable of bond formation with a gaseous or surface species. X^* denotes a surface species occupying a surface site. The deposited tungsten atom, incorporated in the surface lattice, will serve as a free surface site in a subsequent adsorption step, i.e., $W^*\equiv{}^*$. Considering the proposition of the elementary reaction steps listed above, the following presumptions were made.

The tungsten surface temperature is sufficiently high for dissociative SiH_4 chemisorption, which produces adsorbed SiH_x fragments ($0<x<3$) and H_2 molecules or adsorbed hydrogen atoms.[17] Subsequent dissociation of SiH_x^* surface species proceeds on the tungsten surface.

WF_6 molecules chemisorb on the tungsten surface. However, the stepwise dissociation of the admolecules to WF_y^* ($y<5$), as proposed by Arora and Pollard,[16] is assumed to be slow compared to the other steps of the mechanism.

The silicon-hydrogen bond present in the reaction product $SiHF_3$ originates from the reactant molecule SiH_4. Complete dissociation of SiH_4, producing adsorbed Si atoms, and addition of a hydrogen atom at a later stage is thermodynamically unfavorable, since silicon-fluorine bonds (bond energy $\cong$ 600 kJ/mol) are considerably stronger than silicon-hydrogen bonds (bond energy $\cong$ 100 kJ/mol).

Equation (10) is not likely to represent an elementary surface reaction in the mechanism. Instead, an equilibrium may be involved:

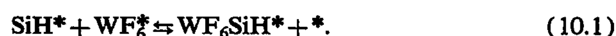

$$SiH^*+WF_6^*\leftrightarrows WF_6SiH^*+{}^*. \tag{10.1}$$

The hypothetical WF_6SiH^* surface species contains one or more Si—F—W bridge bonds, formed as a result of the strong affinity of silicon towards fluorine. Reents, Mandich, and Bondybey[18] proposed the formation of a fluorine-bridged intermediate as the first step in the reaction of WF_6 with silicon clusters. They assume that the initial association reaction, i.e., bonding of silicon through a bridging fluorine to tungsten, is followed by decomposition of the intermediate and formation of silicon fluorides. A fluorine-bridged intermediate WF_6SiH^* is assumed to be involved in the present surface reaction mechanism. We will not attempt to define the detailed structure of the intermediate. If the formation of three fluorine bridge bonds occurs, it may be represented by the formula $WF_3(SiHF_3)^*$. The adduct decomposes according to

$$WF_6SiH^*\leftrightarrows SiHF_3(g)+WF_3^*, \tag{10.2a}$$

and the WF_3^* species will subsequently be consumed by SiH^* species,

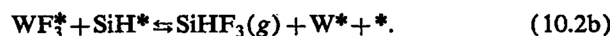

$$WF_3^*+SiH^*\leftrightarrows SiHF_3(g)+W^*+{}^*. \tag{10.2b}$$

Reactions (10.2a) and (10.2b) represent the final elementary steps of the first tentative pathway. In the second pathway steps (5)–(10.1) are the same, whereas WF_6SiH^* itself reacts with another SiH^* species,

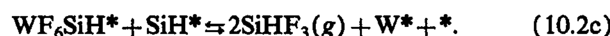

$$WF_6SiH^*+SiH^*\leftrightarrows 2SiHF_3(g)+W^*+{}^*. \tag{10.2c}$$

If steps (5)–(10.1) are all assumed to attain equilibrium, and one of the elementary steps (10.2a) or (10.2c) is rate limiting, equations can be derived expressing the deposition rate as a function of observables $p(SiH_4)$, $p(WF_6)$, and $p(H_2)$ for both pathways. The surface is assumed to be predominantly covered by WF_6^* species. The concentration of free surface sites is approximated by

$$[*]=\frac{1}{1+K_{WF_6}p(WF_6)}, \tag{11}$$

where K_{WF_6} is the equilibrium constant of WF_6 chemisorption.

At high $p(WF_6)$ and low $p(SiH_4)$ the SiH^* concentration is low. Consequently, step (10.2a) is fast compared to step (10.2c) and the first pathway will dominate. The rate is proportional to the surface concentration of WF_6SiH^*. Assuming $K_{WF_6}p(WF_6) \gg 1$, the overall rate equation becomes

$$R=k\{T\}[p(SiH_4)]^1[p(WF_6)]^0[p(H_2)]^{-1.5}, \tag{12}$$

where $k\{T\}$ represents the reaction-rate constant which depends on temperature, the activation energy of the rate-limiting step, and several adsorption and dissociation enthalpies. Apart from the dependence on $p(H_2)$, Eq. (12) is consistent with our observed growth rates at $p(SiH_4)/p(WF_6)<0.3$ (region I).

Increasing the ratio $p(SiH_4)/p(WF_6)$ results in higher SiH^* surface concentrations, and the rate of step (10.2c) will become sufficiently high to compete with (10.2a). As (10.2c) becomes the dominant reaction path, the overall rate equation will be

Downloaded 22 Feb 2005 to 130.161.132.34. Redistribution subject to AIP license or copyright, see http://jap.aip.org/jap/copyright.jsp

$$R=k\{T\}[p(SiH_4)]^2[p(WF_6)]^{-1}[p(H_2)]^{-3}. \quad (13)$$

Regarding the dependence of the deposition rate on $p(SiH_4)$ and $p(WF_6)$ in Eq. (13), this expression is consistent with the observed behavior at $0.5<p(SiH_4)/p(WF_6)<1.0$ (region II) in our work. However, the significant influence of the hydrogen partial pressure, expected from Eqs. (12) and (13), is not found in our measurements. The absence of a decrease of deposition rate at higher $p(H_2)$ indicates that the presence of H^* or H_2 does not influence the concentration and formation of reactive species at the surface. Indeed, Sault and Goodman[17] observed that the rate of dissociative SiH_4 chemisorption is not affected by the presence of adsorbed hydrogen atoms on a W(110) surface. Since silicon is more strongly bound to the tungsten surface than hydrogen, the latter is displaced from the surface by SiH_4. Hence, hydrogen has no influence on the concentrations of Si- or W-containing adspecies. Consequently, steps (5)–(8) are considered to be irreversible; however, as a result of this assumption, the surface concentrations of the H^* and SiH_x^* adspecies can no longer be expressed in terms of the adsorption equilibria of their corresponding gas-phase species. Hence, steady-state approximations, instead of Langmuir–Hinshelwood assumptions, should be employed in order to derive theoretical rate equations. This approach involves a more detailed analysis of the rates of all elementary reaction steps, according to the procedure outlined by Arora and Pollard.[16] However, as we have mentioned above, application of this procedure is beyond the scope of the present work. Here, we only note that the negligible influence of $p(H_2)$ on the deposition rate might be predicted from steady-state approximations.

The reaction mechanism presented in this article should be regarded as a first attempt to explain our observations. It has been formulated within the framework of the Langmuir–Hinshelwood model. The predicted kinetic behavior changes if adspecies are assumed to occupy more than one surface site. For instance, if WF_6 and WF_6SiH adspecies occupy two surface sites, i.e., WF_6 is chemisorbed as WF_6^{**}, the kinetic order in $p(WF_6)$ will be higher than the order in case of single-site adsorption. Consequently, the order in $p(WF_6)$ in case of double-site adsorption does not agree with our experimental observations. Details of these calculations will be given elsewhere.[19] Adsorption on single sites adequately models the dependence of the deposition rate on $p(WF_6)$.

V. CONCLUSIONS

The kinetics of the tungsten LPCVD process using WF_6 and SiH_4 are determined by the partial pressure ratio of the reactant gases. At low ratios, i.e., $p(SiH_4)/p(WF_6)<0.3$, the surface concentration of Si-containing adspecies is relatively low, and the surface is predominantly covered by WF_6. A first order in $p(SiH_4)$ and zeroth order in $p(WF_6)$ are observed in this region. Increasing the ratio to values $0.5<p(SiH_4)/p(WF_6)<1$ results in higher concentrations of Si-containing adspecies; however, WF_6 remains the dominant adspecies. The kinetics become second order in $p(SiH_4)$ and minus first order in $p(WF_6)$. The presence of hydrogen in the reactant mixture has no effect on the deposition rate.

Two surface reaction pathways have been proposed to account for the observation of two kinetic regimes. A Langmuir–Hinshelwood model has been formulated as a first attempt to elucidate the underlying mechanisms. Within this model, the second order with respect to $p(SiH_4)$ is obtained by assuming two Si-containing adspecies to be involved in the rate-determining step. Moreover, the adsorption of hydrogen on the growing surface is considered to be weak compared to adsorption of other species. Hence, hydrogen will not affect the surface concentrations of Si- and W-containing adspecies.

ACKNOWLEDGMENTS

This research is financed partly by the Netherlands Ministry of Economic Affairs in the framework of the Innovation Directed Research Programme for IC Technology (IOP-IC). The authors gratefully acknowledge C.I.M.A. Spee of the Netherlands Organization of Applied Scientific Research for microbalance-weight-measurement software.

[1] E. K. Broadbent and W. T. Stacey, Solid State Technol. 28, 51 (1985).
[2] R. S. Blewer, Solid State Technol. 29, 117 (1986).
[3] R. A. Levy and M. L. Green, J. Electrochem. Soc. 134, 37C (1987).
[4] Y. Kusumoto, K. Takakuwa, H. Hashinokuchi, T. Ikuta, and I. Nakayama, in *Tungsten and Other Refractory Metals for VLSI Applications III*, edited by V. A. Wells (Materials Research Society, Pittsburgh, PA, 1988), p. 103.
[5] M. L. Yu, B. J. Eldridge, and R. V. Joshi, in *Tungsten and Other Refractory Metals for VLSI Applications IV*, edited by R. S. Blewer and C. M. McConica (Materials Research Society, Pittsburgh, PA, 1989), p. 221.
[6] M. L. Yu and B. J. Eldridge, J. Vac. Sci. Technol. A 7, 625 (1989).
[7] N. Kobayashi, H. Goto, and M. Suzuki, in *Proceedings of the 11th International Conference on CVD*, edited by K. E. Spear and G. W. Cullen (The Electrochemical Society, Pennington, NJ, 1990), p. 434.
[8] N. Kobayashi, H. Goto, and M. Suzuki, J. Appl. Phys. 69, 1013 (1991).
[9] J. E. J. Schmitz, A. J. M. van Dijk, and M. W. M. Graef, in *Proceedings of the 10th International Conference on CVD*, edited by G. W. Cullen (The Electrochemical Society, Pennington, NJ, 1987), p. 625.
[10] R. S. Rosler, J. Mendonca, and M. J. Rice, J. Vac. Sci. Technol. B 6, 1721 (1988).
[11] H. L. Park, S. S. Yoon, C. O. Park, and J. S. Chun, Thin Solid Films 181, 85 (1989).
[12] H. Gokce, T. Sahin, and J. T. Sears, in *Tungsten and Other Advanced Metals for VLSI/ULSI Applications V*, edited by S. S. Wong and S. Furukawa (Materials Research Society, Pittsburgh, PA, 1990), p. 103.
[13] J. E. J. Schmitz, M. J. Buiting, and R. C. Ellwanger, in *Tungsten and Other Refractory Metals for VLSI Applications IV*, edited by R. S. Blewer and C. M. McConica (Materials Research Society, Pittsburgh, PA, 1989), p. 27.
[14] M. Suzuki, N. Kobayashi, K. Mukai and S. Kondo, J. Electrochem. Soc. 137, 3213 (1990).
[15] R. V. Joshi, V. Prasad, L. Krusin-Elbaum, M. Yu, and M. Norcott, J. Appl. Phys. 68, 5625 (1990).
[16] R. Arora and R. Pollard, J. Electrochem. Soc. 138, 1523 (1991).
[17] A. G. Sault and D. W. Goodman, Surf. Sci. 235, 28 (1990).
[18] W. D. Reents, Jr., M. L. Mandich, and V. E. Bondybey, Chem. Phys. Lett. 131, 1 (1986).
[19] J. A. M. Ammerlaan, thesis, Delft University of Technology (to be published).

Downloaded 22 Feb 2005 to 130.161.132.34. Redistribution subject to AIP license or copyright, see http://jap.aip.org/jap/copyright.jsp